

## ARTICLE

# Deep-intronic *ATM* mutation detected by genomic resequencing and corrected *in vitro* by antisense morpholino oligonucleotide (AMO)

Simona Cavalieri<sup>1</sup>, Elisa Pozzi<sup>1</sup>, Richard A Gatti<sup>2</sup> and Alfredo Brusco<sup>\*,1</sup>

Recent development of next-generation DNA sequencing (NGS) techniques is changing the approach to search for mutations in human genetic diseases. We applied NGS to study an A-T patient in which one of the two expected mutations was not found after DHPLC, cDNA sequencing and MLPA screening. The 160-kb *ATM* genomic region was divided into 31 partially overlapping fragments of 4–6 kb and amplified by long-range PCR in the patient and mother, who carried the same mutation by segregation. We identified six intronic variants that were shared by the two genomes and not reported in the dbSNP(132) database. Among these, c.1236-405C>T located in IVS11 was predicted to be pathogenic because it affected splicing. This mutation creates a cryptic novel donor (5') splice site (score 1.00) 405 bp upstream of the exon 12 acceptor (3') splice site. cDNA analysis showed the inclusion of a 212-bp non-coding 'pseudoexon' with a premature stop codon. We validated the functional effect of the splicing mutation using a minigene assay. Using antisense morpholino oligonucleotides, designed to mask the cryptic donor splice-site created by the c.1236-405C>T mutation, we abrogated the aberrant splicing product to a wild-type *ATM* transcript, and *in vitro* reverted the functional *ATM* kinase impairment of the patients' lymphoblasts. Resequencing is an effective strategy for identifying rare splicing mutations in patients for whom other mutation analyses have failed (DHPLC, MLPA, or cDNA sequencing). This is especially important because many of these patients will carry rare splicing variants that are amenable to antisense-based correction.

*European Journal of Human Genetics* (2013) 21, 774–778; doi:10.1038/ejhg.2012.266; published online 5 December 2012

**Keywords:** *ATM*; ataxia-telangiectasia; next-generation sequencing; antisense oligonucleotide; deep intronic mutations

## INTRODUCTION

Ataxia-telangiectasia (A-T) is a rare autosomal recessive neurodegenerative disorder (A-T; MIM# 208900) characterized by progressive cerebellar degeneration, oculocutaneous telangiectasia, immunodeficiency, increased cancer risk, sensitivity to ionizing radiation, and chromosomal instability.<sup>1</sup> A-T is caused by mutations in the *ATM* gene (MIM#607585) that encodes a 370-kDa ubiquitous protein. *ATM* is a serine/threonine kinase involved in cell cycle checkpoints, repair of double-strand DNA breaks, response to oxidative stress, and apoptosis.<sup>2,3</sup> More than 600 unique *ATM* mutations have been identified worldwide (www.LOVD.nl/ATM). The majority lead to absence of *ATM* protein and loss of its kinase function. Conventional methods for mutation detection are on the basis of PCR amplification of *ATM* exons, accompanied by MLPA to detect large genomic deletions or duplications.<sup>4,5</sup> This multistep approach identified >95% of the mutations. The application of the next-generation DNA sequencing technology (NGS) is becoming an important tool to identify additional rare mutations. Here, we report the study of an A-T patient with a nonsense mutation in exon 45 and a novel pseudoexon-retaining deep-intronic mutation, detected by genomic resequencing. With the use of antisense morpholino oligonucleotides (AMO) targeted to the aberrant splice-site, we were able to restore normal *ATM* splicing and induce significant amounts of full-length functional *ATM* kinase.

## MATERIALS AND METHODS

### Samples and mutation detection

Samples from patient AT-34-TO and her parents were collected during a diagnostic evaluation by *ATM* molecular screening for suspected A-T. Total genomic DNA was extracted using the Qiaamp DNA mini kit (Qiagen, Mannheim, Germany) from peripheral blood. A lymphoblastoid cell line was established from patient's blood. Initial genetic analyses included short tandem repeats and SNP haplotyping, to detect known Italian founder mutations, DHPLC, and MLPA.<sup>6</sup> *ATM* cDNA amplification and sequencing was performed, as described in.<sup>7</sup> Western blot analysis of *ATM* protein was performed from nuclear protein extracts of patient's lymphoblasts, as described below.

Reference sequence of the *ATM* gene as follows: NM\_000051.3.

### Resequencing of the *ATM* genomic region

The entire 160-kb *ATM* genomic region was divided in 31 partially overlapping fragments of 4–6 kb and amplified by long-range PCR in the patient and her mother (see Supplementary table 1, and Figure 1). PCR was performed in a total volume of 50  $\mu$ l with a final concentration of 200 nM of each primer, 400  $\mu$ M of dNTPs, 1  $\times$  enzyme buffer and 2.5 units of LA polymerase (Takara Bio Inc., Otsu, Shiga 520–2193, Japan), under the following cycling parameters: 1 min at 94 °C, followed by 30 cycles of 10 s at 94 °C, and 1 min/kb at the annealing temperature (see Supplementary table 1), final extension 72 °C for 10 min. Amplicons were run on a TBE-agarose 0.6% gel and UV visualized after ethidium bromide staining to verify product quality, and quantified twice

<sup>1</sup>Università di Torino, Department of Medical Sciences & Azienda Ospedaliera "Città della Salute e della Scienza", Torino, Italy; <sup>2</sup>Department of Pathology and Laboratory Medicine and Human Genetics & David Geffen School of Medicine at UCLA, Los Angeles, CA, USA

\*Correspondence: Dr A Brusco, Università di Torino, Department of Medical Sciences, via Santena 19, Torino 10126, Italy. Tel: +39 11 6334480;

Fax: +39 11 6705668; E-mail: alfredo.brusco@unito.it

Received 25 July 2012; revised 22 October 2012; accepted 1 November 2012; published online 5 December 2012

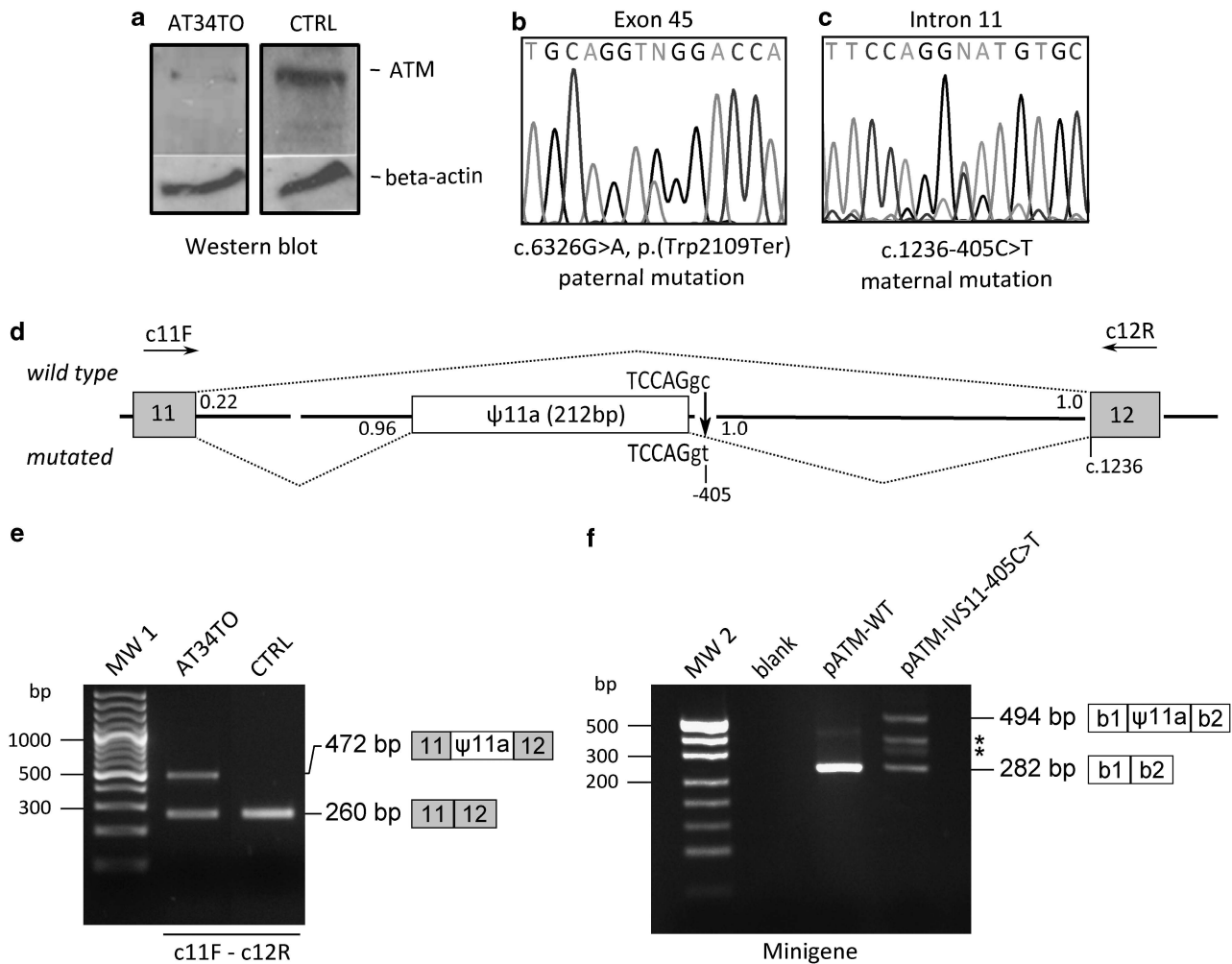


**Figure 1** Mutation detection and cDNA analysis of the deep intronic mutation. (a) Western blot analysis of ATM protein showed reduced levels in AT34TO compared with healthy controls. (b) DHPLC/sequencing allowed the identification of a paternal mutation in exon 45 (c.6326G>A, p.(Trp2109Ter)). (c) Resequencing of the entire *ATM* genomic region allowed the maternal mutation c.1236-405C>T to be located in intron 11. (d) Schematic representation of intron 11 and flanking exons where the deep-intronic mutation c.1236-405C>T is located. This mutation creates a cryptic donor (5') splice-site in intron 11 and results in the inclusion of a pseudoexon of 212 bp in mRNA. (e) cDNA amplification with primers c11F and c12R showed the wild-type band of 260 bp and an extra band of 472 bp containing the pseudoexon. (f) A minigene construct was constructed by subcloning 593 bp of intron 11 into pSPL3 vector. RT-PCR using internal primers of the vector showed only one band of 282 bp in wild type (pATM-WT) corresponding to the synthetic exons b1- b2 of pSPL3; the plasmid containing the mutation (pATM-c.1236-405C>T) gave a normal 282-bp band and an upper band of 494 bp corresponding to the insertion of the 212-bp pseudoexon presented in the mutated clone only. Asterisks indicate bands probably because of minor alternative splice-sites products. MW1: 100-bp ladder plus (Fermentas); MW2: pUC19/Mspl (Fermentas). CTRL: normal control.

using a Qubit fluorimeter (Life Technologies, Carlsbad, CA, USA). A total of 20  $\mu$ g of a pool containing equimolar amounts of each amplified fragment, was resuspended in RNase free water at a concentration of 200 ng/ml and delivered to the Base Clear custom sequencing service (Leiden, The Netherlands). Briefly PCR amplified DNA was fragmented by sonication, gel purified, ligated to adaptors, and sequenced after bridge amplification using an Illumina Genome Analyzer IIX as paired-end 50-bp reads (Illumina, San Diego, CA, USA). Sequencing data were filtered for low-quality reads, exported as FASTAQ files and aligned against the *ATM* reference sequence (Ref Seq NG\_009830.1) using the CLCbio 'Map reads to reference' software. The average coverage depth was 300X. All sequence variants shared between the patient and mother were further searched in the dbSNPs 132. Splice site score analysis was performed using Splice Site Prediction software ([http://www.fruitfly.org/seq\\_tools/splice.html](http://www.fruitfly.org/seq_tools/splice.html)).<sup>8</sup>

#### cDNA mutation analysis and c.1236-405 C>T mutation screening

Total RNA was extracted using the RNeasy Plus Mini Kit (Qiagen S.r.l, Milano, Italy), and retrotranscribed using the Transcriptor First Strand cDNA Synthesis

kit (Roche Diagnostics, Mannheim, Germany), according to the manufacturer's instructions. To analyze the pseudoexon inclusion, we designed a specific RT-PCR exploiting primers located in exons 11 (c11F: 5'-TCCCTTGCAAAG GAAGAAA-3') and 12 (c12R: 5'-TTTTGTGAGCTTCTAGGTTTGACC-3') of the *ATM* gene (reference sequence: U82828.1). PCR conditions were 0.3  $\mu$ M of each primer, 0.8 mM dNTPs, and 0.5 units of KAPA fast polymerase (KAPA Biosystems, Woburn, MA, USA) in the following cycling conditions: 2 min at 95 °C, followed by 29 cycles 15 s at 95 °C, 15 s at 56 °C, and 45 s at 72 °C; final extension of 1 min at 72 °C.

#### Minigene construction

A minigene assay was set up to test the effect of the *ATM* c.1236-405 C>T (IVS11) on splicing. We amplified a 593-bp genomic fragment from AT34TO, using primers designed with a restriction site (*Eco*RI-forward, 5'-TTGAA CACCTGTTATGGGCTAA-3'; *Bam* HI-reverse, 5'-TGGCTAGCTGGGTAA GCTGT-3'). PCR products were cloned into a pGEM-T Easy Vector (Promega, Madison, WI, USA) and transformed in DH5 $\alpha$  bacterial cells, following the

manufacturer's recommendations (RBC Bioscience, Chung Ho City, Taiwan). Plasmids containing the wild-type or the variant sequence were extracted using the PureYield plasmid system (Promega) and sequence checked. After preparative double-digestion with *EcoRI* and *BamHI* restriction endonucleases, inserts were gel-purified and sub-cloned into a pSPL3 exon-trapping vector (Life Technologies, Paisley, UK). pSPL3 plasmids containing the wild-type (pSPL3\_C) or the variant (pSPL3\_T) sequence were extracted using PureYield Plasmid Midiprep System (Promega), and transfected into HEK293 cells using the TurboFect kit (Fermentas, Vilnius, Lithuania). After 24 h, total RNA was extracted and retrotranscribed with the Cells-To-CT kit (Life Technologies). The presence of the pseudoexon was verified by cDNA amplification using vector primers (5'-TCTGAGTCACCTGGACAACC-3'; 5'-ATCTCAGTGG-TATTTGTGAGC-3').

### Correction of *ATM* pre-mRNA splicing by AMO

The 25-mer AMO, 5'-GGGCATGGTGGCACATACCTGGAAT-3' (mutation underlined) was designed to target the aberrant donor splice site activated by the c.1236-405 C>T mutation. The AMO was synthesized and purified by Gene Tools (LLC, Philomath, OR, USA). Treatment of LCLs with AMO was performed, as previously described by Du *et al.*<sup>14</sup> Briefly,  $5 \times 10^5$  LCLs cells were resuspended in 0.5 ml 5% FBS/RPMI 1640 medium and AMO was added directly to the medium at the concentration indicated. Endo-Porter (Gene Tools) was added to the medium to help intracellular corporation of the AMO. A Vivo-AMO (Gene Tools), identical in sequence to the AMO, but bound to a proprietary cell-penetrating peptide, was also used at two different concentrations to enhance cellular delivery. After 48-h incubation, cells were collected and rinsed in PBS. Total RNA was extracted and cDNA retrotranscribed, as described above. For RT-PCR primers c11F and c12R were used to amplify both the full-length and the mutant transcripts.

### Western blot analysis and *ATM* kinase activity

For analysis of AMO-induced *ATM* protein levels, LCLs were treated with various concentrations of Vivo-AMO for 4 days and nuclear extracts were prepared for each sample, according to the NE-PER protocol (Pierce, Rockford, IL, USA). Nuclear protein lysates (20  $\mu$ g), were separated on a 4–12% precast SDS polyacrylamide gel (Bio-Rad, Hercules, CA, USA) and electrotransferred onto nitrocellulose membrane. Membranes were blocked with 5% milk-TBS-0.1% Tween-20 and incubated overnight at 4°C with anti-*ATM* antibody (ab17995, Abcam, Cambridge, UK) at 1:5000 dilution.

To test *ATM* kinase activity, patient lymphoblastoid cells, treated or untreated with vivo-AMO, were irradiated with 10-Gy gamma irradiation to induce DNA damage (Radgil, Gilardoni Instruments, Mandello del Lario, Lecco, Italy) and incubated at 37°C for 30 min before protein extraction. SMC1 phosphorylation was verified using an anti-SMC-Phospho Ser966 (ab1276 Abcam) at 1:2000 dilution. Images were acquired and quantified using a Chemidoc apparatus and ImageLab software (Bio-Rad).

## RESULTS

### Clinical description

Clinical diagnosis of AT34TO was on the basis of presence of progressive cerebellar ataxia, oculocutaneous telangiectasias, immunodeficiency, and increased serum alpha fetoprotein, and <3–5% *ATM* protein on western blot (Figure 1a). AT34TO was of special interest. Initial presentation of ataxia was at 7 year. The patient walked with minimal assistance until 14 year. She has no history of pulmonary or bronchial infections. A previous genetic screening by DHPLC analysis allowed us to identify a mutation, c.6326G>A in exon 45 that created a stop codon at amino acid 2109 [p.(Trp2109Ter)], of paternal origin (Figure 1b). This result suggested that the small amount of *ATM* protein present in the patient might reflect the influence of the unidentified maternal mutation. We suspected a deep intronic mutation, but cDNA analysis failed to identify anomalous band shifts.

### Identification of a deep intronic mutation

Resequencing of the entire 160-kb *ATM* genomic region allowed the identification of 24 intronic nucleotide variants shared in heterozygosis between the proband and her mother. Among the six unreported in the dbSNPs (ver. 132), c.1236-405C>T (coverage 670X) was the only one predicted to be pathogenic because it affected splicing (BDGP, www.fruitfly.org/seq)(Figure 1c). c.1236-405C>T, located in intron 11, was predicted to activate a donor (5') splice site (scheme in Figure 1d). cDNA analysis with primers c11F and c12R (Figure 1d) showed a normal band of 260 bp and a larger mutated molecular band of 472 bp (Figure 1e). Direct sequencing showed the 472-bp band included a 212 bp pseudoexon derived from intron 11 (see scheme in Figure 1d).

### Minigene assay

A minigene construct was prepared by cloning 593 bp of genomic DNA centered on the genomic change c.1236-405C>T, and a wild-type sequence control, into the pSPL3 vector (Figure 1f). These showed the post-transfection spliced products of wild-type pATM-WT, 282 bp, corresponding to the normal spliced product (exon b1/exon b2); pATM-IVS11-405C>T containing the mutated allele showed the 282-bp band and a larger band of 494 bp. The latter sequence analysis contained the 212-bp pseudoexon. Additional bands (asterisks) likely indicate heteroduplexes or alternative splicing products.

### Correction of *ATM* Pre-mRNA splicing mutation using AMO

We designed an antisense morpholino oligonucleotide (AMO) to mask the 5'cryptic donor splice-site created by the c.1236-405C>T mutation and restore the normal wild-type splicing (Figure 2a).

Patient LCLs were treated with 0, 20, 40, 50  $\mu$ M concentrations of neutral AMO for 48 h; total RNA was isolated and RT-PCR was performed using the strategy in Figure 1d. The wild-type and mutant band ratio is ~50% in untreated cells. At the highest 50  $\mu$ M concentration, neutral-AMO treatment showed a ~26% increase of the wild type 260-bp band, corresponding to normal splicing, vs the 472-bp mutant (Figure 2b). To enhance the delivery and efficiency of the AMO, we also designed a structurally modified Vivo-AMO that dramatically improved the induction of wild-type transcript. We showed that at 1  $\mu$ M concentration, the wild-type band intensity was increased by 50%, whereas at 2  $\mu$ M, the mutant band had almost disappeared, suggesting a complete abrogation of the aberrant splicing (Figure 2c). To determine the effect of Vivo-AMO on the protein level, we performed a western blot on nuclear extracts of LCLs after 4 days exposure. A significant amount of functional *ATM* protein was induced even at the lower dose of 1  $\mu$ M and reached a maximum of ~50% of WT levels at 2  $\mu$ M (Figure 2d). After 84-h treatment, we noticed a mild Vivo-AMO toxicity at 2  $\mu$ M working concentration (data not shown). Cell viability was reduced to 87% and 68% in cells treated with 1  $\mu$ M and 2  $\mu$ M Vivo-AMO, respectively.

### Restoration of *ATM* kinase activity in AMO-treated cells

To assess the enzymatic activity of the AMO-induced *ATM* protein, we irradiated at 10 Gy patient's LCLs, after 84-h treatment with and without Vivo-AMO, and measured the phosphorylation of the *ATM* substrate SMC1 at Ser-966. As showed in Figure 2e, no IR-induced phosphorylation was observed in untreated AT34TO cells, whereas phosphorylation of LCLs treated with both 1 and 2  $\mu$ M Vivo-AMO was comparable with WT levels.

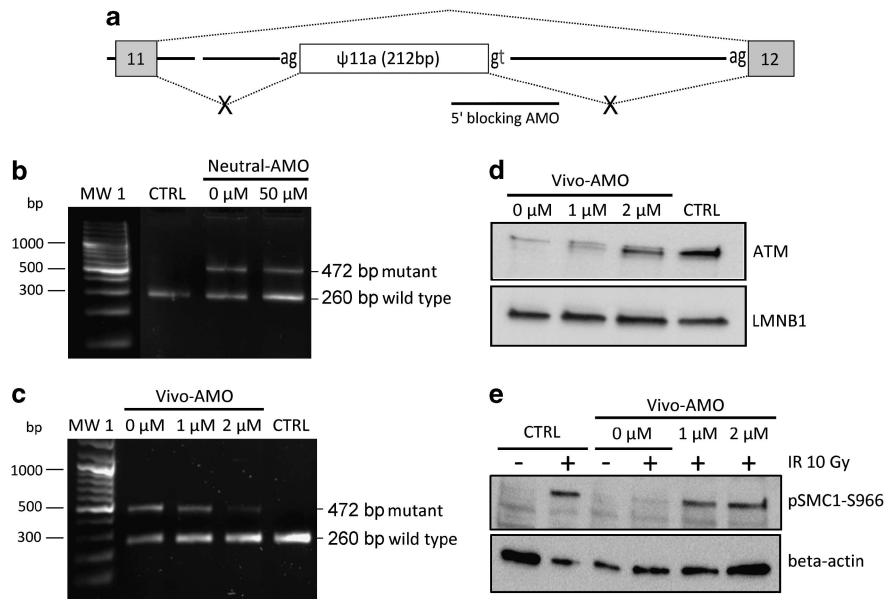


**Figure 2** Correction of splicing mutation using AMO. (a) Schematic representation of the AMO strategy and location of the 5'-blocking AMO. (b,c) Patient's LCLs were treated for 48 h with a maximum of 50  $\mu\text{M}$  neutral-AMO and with 1 and 2  $\mu\text{M}$  of vivo-AMO that dramatically improved *ATM* splicing correction efficiency of pre-mRNA. (d, e) Immunoblots demonstrate the restoration of *ATM* protein levels and its kinase activity after AMO. Cells were exposed to 1 and 2  $\mu\text{M}$  vivo-AMO for 84 h before nuclear lysates were isolated for western blots. AMO-treated cells were harvested 30 min after irradiation damage (10 Gy) to activate *ATM* kinase. Nuclear lysates were isolated to analyze SMC1-S966 phosphorylation. Nuclear extracts from normal cells were used as controls. Beta-actin was used as loading controls. MW1: 100 bp ladder plus (Fermentas). CTRL: normal control.

## DISCUSSION

According to 'The Human Gene Mutation Database' (<http://www.hgmd.org/>), ~10% of reported mutations in disease-associated genes are splicing mutations. Although most of them affect consensus sites, deep intronic mutations are increasingly being reported in human diseases, as we have recently shown in megalencephalic leukoencephalopathy.<sup>9</sup> Such mutations are easily missed because they are not targeted by standard genetic screening, and are not detected by the more recent whole-exome sequencing technique. NGS of the entire genomic region of a gene is a plausible next alternative for identifying rare mutations whenever DHPLC, MLPA, and cDNA sequencing are unrevealing.

Deep-intronic mutations are particularly interesting from a therapeutic point of view. In case of a deep-intronic mutation, the wild-type downstream splice sites remain unchanged, and thus can be utilized to force the cell to skip the pseudoexon. Such achievement may be obtained using antisense oligonucleotides (AONs) that, targeting the donor or acceptor site of the pre-mRNA, cause the skipping of the relevant pseudoexon. The rescue of splicing defects has been demonstrated both *in vitro* and *in vivo*, and clinical trials are already in phase II, as shown by Duchenne muscular dystrophy studies.<sup>10,11</sup> This strategy has already found a proof of principle in the *ATM* gene where approximately half of unique mutations are splicing mutations.<sup>12,13</sup> In particular, some of these mutations have been demonstrated to occur in deep intronic regions that are associated with the retention of intronic sequences in the mRNAs and AONs have been already designed to successfully abrogate these *ATM* mutations.<sup>5,14</sup>

In the current study, we studied a new deep-intronic mutation detected in an A-T patient using a NGS strategy to resequence the entire 160-kb *ATM* genomic region, after standard mutation detection techniques (DHPLC, MLPA and cDNA sequencing), failed to identify the second mutation. Our strategy to sequence the proband and the

transmitting parent, in our case the mother, was very successful. The single-nucleotide change (c.1236-405C>T) was novel and had not been reported in the dbSNP. It was predicted to be pathogenic for splicing within intron 11. The mutation created a new cryptic 5'ss with a strength of 1.00 and activated a cryptic 3'ss site 212 bp upstream with a strength of 0.96.

Complementary DNA analysis failed to identify the pseudoexon. This is likely because of unbalanced amplification in favor of the normal vs the mutated larger fragment, and may also reflect the effect of nonsense mediated decay, considering that the pseudoexon contains multiple premature stop codons.<sup>15</sup> Using a minigene construct, we demonstrated that mutation c.1236-405C>T alters a donor splice site, because it causes the inclusion of the pseudoexon only in the transcript from the plasmid carrying the mutation. Indeed, a residual amount of normal splice product is present even in the presence of the mutation, suggesting that it behaves as a leaky mutation. This is in agreement with a residual amount of *ATM* protein seen in patient's western blot and slow progression of neurological symptoms.

To restore normal *ATM* splicing at the pre-mRNA level, we targeted a specific AMO to the aberrant splice site mutation. The efficiency of *ATM* correction was 26% with 50  $\mu\text{M}$  neutral-AMO and varied from 50% to almost 95% with Vivo-AMO, depending on the concentrations used (1 and 2  $\mu\text{M}$ ). For restoration of *ATM* protein level, we reached ~50% at 84 h after 2- $\mu\text{M}$  Vivo-AMO exposure. The restored *ATM* protein was functional for kinase activity, as assessed by phosphorylation of SMC1 after IR exposure, even at the lower dose of Vivo-AMO.

Published data estimate that a subset of A-T patients with functional *ATM* protein levels around 5–20% has a milder phenotype, with later onset and slower progression of neurological symptoms.<sup>16</sup> Considering that obligate *ATM* heterozygotes have 40–50% of normal *ATM* protein levels and do not show any sign of disease,<sup>17</sup> we have



hypothesized that even a minimal rescue of functional ATM protein levels could provide therapeutic benefit in A-T patients. It remains undetermined, however, whether A-T patients can recover from long-standing cerebellar damage. This question might be resolved by clinical trials of AON that would treat A-T patients of various ages and clinical severity.

Chemically modified (Vivo) AMOs strongly enhance cell-delivery and efficiency. However, working concentrations of Vivo-AMO (2  $\mu$ M) are toxic for cells. Therefore, future applications will require new AON derivatives (eg, 2'-O-Methyl-Phosphorotioate).

Overall, we consider that NGS resequencing is feasible and affordable for clinical purposes. We calculate a total cost of 1500 Euros for NGS reagents, and this cost will most likely decrease in the near future.

### CONFLICT OF INTEREST

The authors declare no conflict of interest.

### ACKNOWLEDGEMENTS

This work was supported by the Associations 'Un vero sorriso', 'Gli Amici di Valentina', and 'Noi per Lorenzo'.

- 1 Gatti RA: Ataxia-Telangiectasia; in: Scriver CRB AL, Sly WS, Valle D (eds) *The Metabolic and Molecular Bases of Inherited Disease*. New York: McGraw-Hill, 2001, pp 705–732.
- 2 Lavin MF, Spring K: Upregulation of Fas and apoptosis in thymic lymphomas in Atm knock-in mice. *Toxicology* 2002; **181-182**: 483–489.
- 3 Shiloh Y: The ATM-mediated DNA-damage response: taking shape. *Trends Biochem Sci* 2006; **31**: 402–410.

- 4 Cavalieri S, Funaro A, Porcedda P *et al*: ATM mutations in Italian families with ataxia telangiectasia include two distinct large genomic deletions. *Hum Mutat* 2006; **27**: 1061.
- 5 Nakamura K, Du L, Tunuguntla R *et al*: Functional characterization and targeted correction of ATM mutations identified in Japanese patients with ataxia-telangiectasia. *Hum Mutat* 2012; **33**: 198–208.
- 6 Cavalieri S, Funaro A, Pappi P, Migone N, Gatti RA, Brusco A: Large genomic mutations within the ATM gene detected by MLPA, including a duplication of 41kb from exon 4–20. *Ann Hum Genet* 2008; **72**: 10–18.
- 7 Coutinho G, Xie J, Du L, Brusco A, Krainer AR, Gatti RA: Functional significance of a deep intronic mutation in the ATM gene and evidence for an alternative exon 28a. *Hum Mutat* 2005; **25**: 118–124.
- 8 Reese MG, Eeckman FH, Kulp D, Haussler D: Improved splice site detection in Genie. *J Comput Biol* 1997; **4**: 311–323.
- 9 Mancini C, Vaula G, Scalzitti L *et al*: Megalencephalic leukoencephalopathy with subcortical cysts type 1 (MLC1) due to a homozygous deep intronic splicing mutation (c.895-226T>G) abrogated *in vitro* using an antisense morpholino oligonucleotide. *Neurogenetics* 2012; **13**: 205–214.
- 10 Aartsma-Rus A, den Dunnen JT, van Ommen GJ: New insights in gene-derived therapy: the example of Duchenne muscular dystrophy. *Ann N Y Acad Sci* 2010; **1214**: 199–212.
- 11 Lu QL, Yokota T, Takeda S, Garcia L, Muntoni F, Partridge T: The status of exon skipping as a therapeutic approach to duchenne muscular dystrophy. *Mol Ther* 2011; **19**: 9–15.
- 12 Teraoka SN, Telatar M, Becker-Catania S *et al*: Splicing defects in the ataxia-telangiectasia gene, ATM: underlying mutations and consequences. *Am J Hum Genet* 1999; **64**: 1617–1631.
- 13 Concannon P, Gatti RA: Diversity of ATM gene mutations detected in patients with ataxia-telangiectasia. *Hum Mutat* 1997; **10**: 100–107.
- 14 Du L, Pollard JM, Gatti RA: Correction of prototypic ATM splicing mutations and aberrant ATM function with antisense morpholino oligonucleotides. *Proc Natl Acad Sci USA* 2007; **104**: 6007–6012.
- 15 Holbrook JA, Neu-Yilik G, Hentze MW, Kulozik AE: Nonsense-mediated decay approaches the clinic. *Nat Genet* 2004; **36**: 801–808.
- 16 Gilad S, Chessa L, Khosravi R *et al*: Genotype-phenotype relationships in ataxia-telangiectasia and variants. *Am J Hum Genet* 1998; **62**: 551–561.
- 17 Chun HH, Sun X, Nahas SA *et al*: Improved diagnostic testing for ataxia-telangiectasia by immunoblotting of nuclear lysates for ATM protein expression. *Mol Genet Metab* 2003; **80**: 437–443.

Supplementary Information accompanies the paper on European Journal of Human Genetics website (<http://www.nature.com/ejhg>)